# Allelic mutant series reveal distinct functions for *Arabidopsis* cycloartenol synthase 1 in cell viability and plastid biogenesis

**Elena Babiychuk*†, Pierrette Bouvier-Navé‡, Vincent Compagnon‡, Masashi Suzuki§, Toshiya Muranaka§, Marc Van Montagu*†¶, Sergei Kushnir*†, and Hubert Schaller‡¶**

*Department of Plant Systems Biology, Flanders Institute for Biotechnology, Technologiepark 927, 9052 Ghent, Belgium; †Department of Molecular Genetics, Ghent University, 9052 Ghent, Belgium; ‡Institut de Biologie Moléculaire des Plantes, Centre National de la Recherche Scientifique–Unité Propre de Recherche 2357, Université Louis Pasteur, 28 rue Goethe, 67083 Strasbourg, France; and §RIKEN Plant Science Center, Yokohama, Kanagawa 230-0045, Japan

Contributed by Marc Van Montagu, December 24, 2007 (sent for review August 31, 2007)

**Sterols have multiple functions in all eukaryotes. In plants, sterol biosynthesis is initiated by the enzymatic conversion of 2,3-oxidosqualene to cycloartenol. This reaction is catalyzed by cycloartenol synthase 1 (CAS1), which belongs to a family of 13 2,3-oxidosqualene cyclases in *Arabidopsis thaliana*. To understand the full scope of sterol biological functions in plants, we characterized allelic series of *cas1* mutations. Plants carrying the weak mutant allele *cas1–1* were viable but developed albino inflorescence shoots because of photooxidation of plastids in stems that contained low amounts of carotenoids and chlorophylls. Consistent with the CAS1 catalyzed reaction, mutant tissues accumulated 2,3-oxidosqualene. This triterpenoid precursor did not increase at the expense of the pathway end products. Two strong mutations, *cas1–2* and *cas1–3*, were not transmissible through the male gametes, suggesting a role for CAS1 in male gametophyte function. To validate these findings, we analyzed a conditional *CRE/loxP* recombination-dependent *cas1–2* mutant allele. The albino phenotype of growing leaf tissues was a typical defect observed shortly after the *CRE/loxP*-induced onset of *CAS1* loss of function. In the induced *cas1–2* seedlings, terminal phenotypes included arrest of meristematic activity, followed by necrotic death. Mutant tissues accumulated 2,3-oxidosqualene and contained low amounts of sterols. The vital role of sterols in membrane functioning most probably explains the requirement of CAS1 for plant cell viability. The observed impact of *cas1* mutations on a chloroplastic function implies a previously unrecognized role of sterols or triterpenoid metabolites in plastid biogenesis.**

albinism | sterols | triterpenoid metabolites | 2,3-oxidosqualene

Plant cells use a sterol biosynthetic pathway that is peculiar compared with that of other eukaryotes (1, 2). Animals and fungi cyclize the 30-carbon atom precursor 2,3-oxidosqualene into the tetracyclic triterpene lanosterol, which is metabolized into cholesterol and ergosterol, respectively, whereas plants transform the same precursor into the cyclopropylsterol intermediate cycloartenol, which is converted into sitosterol (Fig. 1). The physiological role of cyclopropylsterol intermediates and the apparent necessity for plants to synthesize sitosterol by the cycloartenol route are not understood. An *Arabidopsis thaliana* cDNA encoding cycloartenol synthase 1 (CAS1) has been cloned by functional expression in an ergosterol auxotroph of yeast (*Saccharomyces cerevisiae*) deficient in lanosterol synthesis (3). CAS1 (At2g07050) belongs to a family of 13 triterpene synthases (4), among which At3g45130 has recently been shown to encode a lanosterol synthase 1 (5, 6). Hence, the first committed step in plant sterol biosynthesis may be functionally redundant, as suggested by the possible existence of a lanosterol route besides the major cycloartenol route to sitosterol (7). Other characterized triterpene synthases, such as LUP1 and LUP2 (Fig. 1), catalyze the formation of nonsteroidal polycyclic triterpenes, among which lupeol and $\beta$-amyrin are common secondary metabolites (8–12).

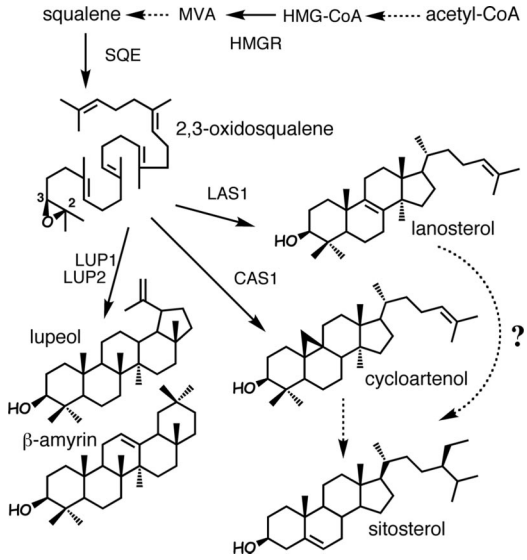


**Fig. 1.** Sterol and nonsteroidal triterpene biosynthetic pathways in plants. HMG-CoA, 3-hydroxy-3-methylglutaryl-CoA; MVA, mevalonate; SQE, squalene epoxidase; LAS1, lanosterol synthase; LUP1 and LUP2, pentacyclic triterpene alcohol synthases.

Molecular genetic analysis of *Arabidopsis* mutants affected in the postsqualene segment of sterol metabolism have uncovered a wide spectrum of developmental abnormalities, such as embryo or seedling lethality (13, 14), dwarfism attributable to brassinosteroid deficiency (15–17), and size variation (18–20), and have provided new insights into the physiological functions of membrane sterols and their role as precursors of the brassinosteroid phytohormones (21–23). To better understand the full scope of sterol biological functions in plant cells, allelic series of *cas1* mutations were analyzed. The data emphasized an essential role of CAS1 for the plant cell viability, suggested the involvement of this enzyme in the regulation of triterpenoid biosyn-

Author contributions: E.B., T.M., M.V.M., S.K., and H.S. designed research; E.B., P.B.-N., V.C., M.S., S.K., and H.S. performed research; E.B., P.B.-N., V.C., M.S., T.M., M.V.M., S.K., and H.S. analyzed data; and E.B., S.K., and H.S. wrote the paper.

The authors declare no conflict of interest.

¶To whom correspondence may be addressed. E-mail: mamon@psb.ugent.be or hubert.schaller@ibmp-ulp.u-strasbg.fr.

This article contains supporting information online at www.pnas.org/cgi/content/full/0712190105/DC1.



PLANT BIOLOGY

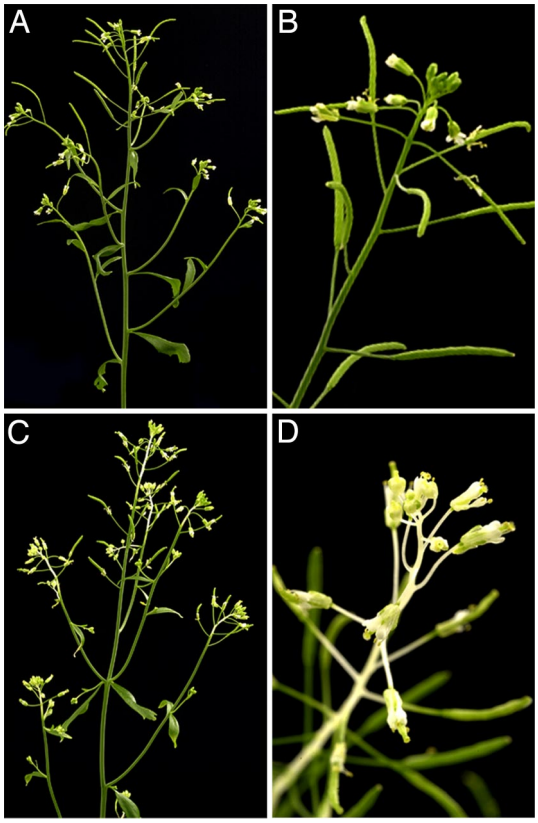


**Fig. 2.** Morphological phenotype of the *cas1–1* mutant. (*A*) Wild-type inflorescence shoot of *Arabidopsis* ecotype C24. (*C*) Inflorescence shoot of the *cas1–1* mutant. (*B* and *D*) Close-ups of inflorescence shoots of wild-type and mutant plants shown in *A* and *C*, respectively.

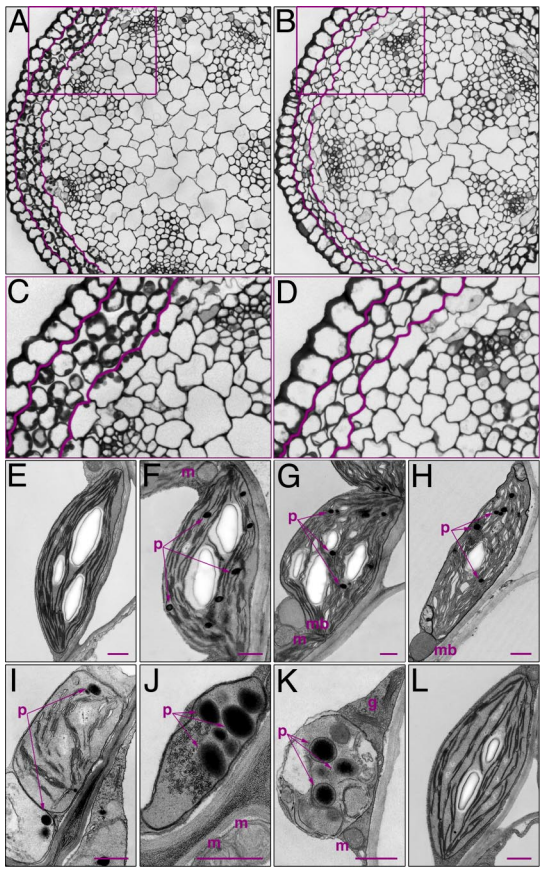


**Fig. 3.** Cellular phenotype of the *cas1–1* mutant. (*A* and *B*) Toluidine blue-stained transverse cross-section of wild-type (*A*) and albino *cas1–1* (*B*) stems. (*C* and *D*) Enlarged parts of images in *A* and *B*. Highlighted are the chlorenchyma subepidermal cell layers with chloroplasts (*C*) and without well differentiated chloroplasts (*D*). (*E*) Plastid morphology in cells from the lower part of wild-type stems, ≈3–5 cm above the rosette. The corresponding stem region in the *cas1–1* mutant is green as well. (*F–K*) Progressive acropetal bleaching of stems correlated with plastid morphology. Thin sections of *cas1–1* stems collected at ≈2-cm intervals showed plastid types in the developmentally oldest cell positioned at the base of the stem, ≈3.5 cm above the rosette (*F*), and the youngest albino cell at the top of the shoot (*K*). Mutant plastids (*I–K*) lack thylakoid membrane system and starch granules and accumulate electron-dense vesicles that may correspond to plastoglobuli. (*L*) Chloroplast in wild-type chlorenchyma cell from distal parts of the stem. g, Golgi apparatus; m, mitochondria; mb, microbody; p, plastoglobuli. (Scale bars, 0.5 $\mu$m.)

thesis, and indicated, to our knowledge, a previously unrecognized role of sterols or their precursors in chloroplast differentiation.

## Results

**The *cas1–1* Mutant of *Arabidopsis* Has an Albino Phenotype Late in Development.** To identify pigment-deficient mutations in genes that encode nonplastidial proteins, we carried out a phenotypic screening of our collection of 402 sequence-indexed, exon-trap lines generated with a T-DNA vector (24). The line L2–19 had a T-DNA insertion within the *CAS1* gene and segregated a characteristic pigment-deficient phenotype of inflorescence shoots (Fig. 2). Albinism affected the flower-carrying parts of the stems. The first 10 to 20 flowers and siliques attached to albino stems had green colored tissues that are normally chlorophyllous in the wild type. Flowers that developed later had either albino or variegated sepals and carpels. Sterility of the purely albino flowers was the probable reason for mutant plants to have, on average, a 2-week longer lifespan than the wild type. Progeny seedlings of homozygous plants showed various developmental abnormalities, such as pigment variegation, polyembryony, fused cotyledons, and multiple cotyledons, reminiscent of phenotypes associated with mutations in sterol biosynthesis (13). Such phenotypes were not observed in the progeny of heterozygous parent plants, suggesting that the maternal tissue provided the CAS1 product to developing embryos.

Light and electron microscopy revealed that cells from three cortical layers just below the epidermis of albino stems did not possess fully differentiated chloroplasts (Fig. 3 *A-D*). These albino mutant cells had plastids that were devoid of the organized system of thylakoid membranes (Fig. 3 *I–K*), which is normally found in fully differentiated plastids from stems of wild types (Fig. 3 *E* and *L*) or green stems of *cas1–1* (Fig. 3 *F–H*). Spectral measurements of pigments indicated that albino parts of *cas1–1* stems had a reduced carotenoid (10-fold) and chlorophyll (12-fold) content compared with that of the wild type [supporting information (SI) Fig. 7], suggesting an impaired carotenoid biosynthesis in the apical part of the stems. To find out whether the mutant chloroplasts had suffered photooxidative damage, mutant plants were grown first at a light intensity of 40–60 $\mu$mol·m$^{-2}$·s$^{-1}$, until the flowering shoots reached a height of 10 to 15 cm, and then at a reduced photon fluence of 5–10 $\mu$mol·m$^{-2}$·s$^{-1}$. Shoots that developed under low-light conditions were able to green, indicating that the albinism of stems was attributable to photooxidative damage of chloroplasts. The albino phenotype cosegregated with the T-DNA in three backcross generations and was genetically complemented by the *CAS1* cDNA expressed from a constitutive 35S cauliflower mosaic virus (CaMV) promoter, demonstrating that the mutant phenotype was caused by the deficiency in the *CAS1* gene function (*SI Methods*).

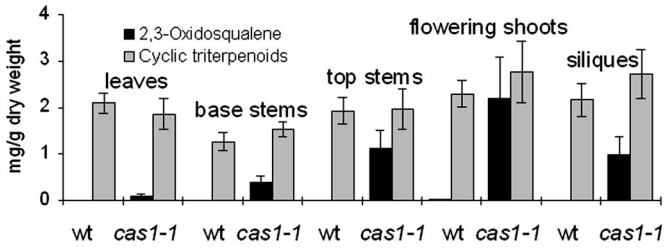


**Fig. 4.** Triterpenoid content of wild-type and *cas1–1* tissues. Samples prepared from tissues of at least 15 individual plants with ≈20 siliques were analyzed. The layout for material collection is detailed in SI Fig. 8. Cyclic triterpenoids are metabolites derived from 2,3-oxidosqualene (see SI Table 1 for details). The data are from three independent experiments.

**Chemical Phenotype of *cas1–1*.** Triterpenoid analysis of wild-type and *cas1–1* plants showed that 2,3-oxidosqualene accumulated in *cas1–1*, a chemical phenotype fully consistent with CAS1 being a functional 2,3-oxidosqualene cyclase *in planta*. The accumulation of 2,3-oxidosqualene in *cas1–1* varied according to organs (Fig. 4 and SI Fig. 8). Rosette leaves contained low amounts, whereas upper stems, flowering shoots, and siliques had the highest quantities of 2,3-oxidosqualene. This accumulation did not occur at the expense of the end products of the cyclic triterpenoid pathway, among which the quantities of total $\Delta^5$ sterols were equivalent in the wild-type and in *cas1–1* (SI Table 1), as was the case in inflorescences of *cas1–1* plants with similar or even larger amounts of cyclic triterpenoids than in the wild type (Fig. 4). To better understand such an apparent increase in the metabolic flux toward total triterpenoids in *cas1–1* flowering shoots, we measured the activity of the enzyme 3-hydroxy-3-methylglutaryl-CoA reductase (HMGR) (Fig. 1), known to be a rate-limiting step in phytosterol accumulation (25–28). HMGR-specific activity in *cas1–1* flowering shoots increased by 30% (5.72 ± 0.1 vs. 4.34 ± 0.25 nmol·mg$^{-1}$ protein per hour in wild type). These results suggested that a higher activity of an enzyme upstream to CAS1 (Fig. 1) may be responsible for the increase of cyclic triterpenoids and could contribute to the dramatic accumulation of 2,3-oxidosqualene in the *cas1–1* mutant.

***CAS1* Is Essential in Plant Cells.** Because CAS1 is thought to be a major 2,3-oxidosqualene cyclase that initiates postsqualene sterol biosynthesis in plants (1, 2, 7) and sterols are known to be essential in yeast, a null mutant allele would be expected to be lethal, given that the CAS1 function is not redundant (2). Indeed, molecular analysis of the *cas1–1* mutation showed that it is a weak allele caused by the T-DNA insertion into the 3′ UTR 177 bp downstream from the translation termination codon TGA and ≈50 bp upstream from the polyadenylation site (Fig. 5*A*), with a lower mRNA expression from the mutated locus as a consequence (Fig. 5*B*). RT-PCR analysis of the *cas1–1* locus suggested that five different CAS1 proteins were synthesized (Fig. 5*C* and SI Table 2), of which one was a wild-type protein and the four others were mutant isoforms with the last seven amino acid residues of CAS1 replaced by amino acid sequences of different lengths. The developmental pattern of the *CAS1* expression was examined by histochemical staining with β-glucuronidase (GUS) in plants that were transformed with a *CAS1* promoter driving the expression of the *uidA* gene of *Escherichia coli*. The transgene was ubiquitously expressed in *Arabidopsis* organs (*SI Methods* and SI Fig. 9). This observation, together with the physiological and chemical phenotypes of *cas1–1*, mostly restricted to inflorescence shoots (Fig. 4), hinted at a possible redundancy of CAS activity in organs, such as leaves.

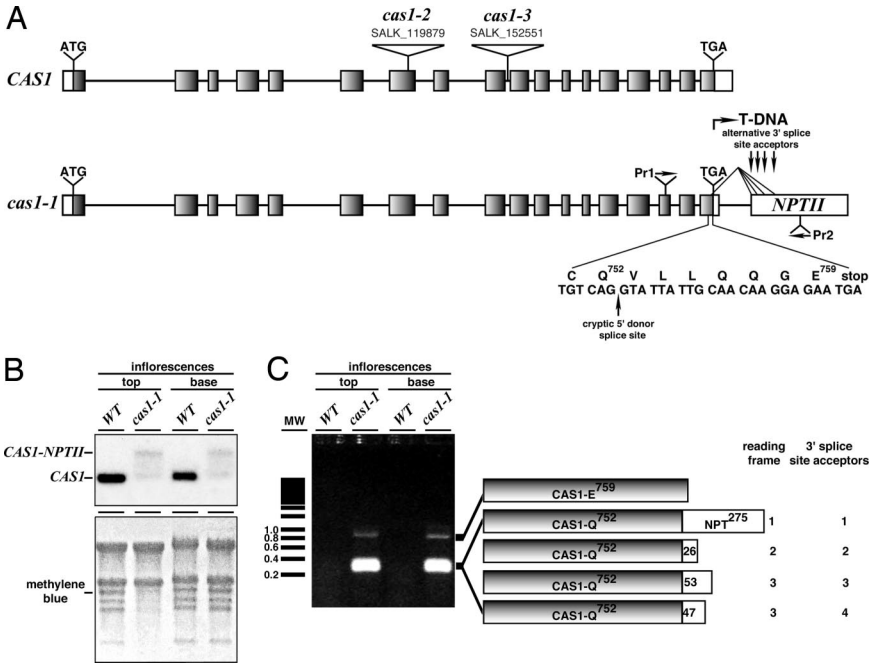


**Fig. 5.** *CAS1* mutant alleles. (*A*) Wild-type (*CAS1*) and mutated loci *cas1–1*, *cas1–2*, and *cas1–3*. Exon-labeled *NPTII* encodes a reading frame for neomycin phosphotransferase that lacks the translation initiation codon (ATG). Heterologous splicing events use the cryptic 5′ splice site donor within *CAS1* exon 18, as indicated, and any one of the four alternative 3′ splice site acceptors from the T-DNA. The T-DNA insertion mutant alleles *cas1–2* (SALK_119879) and *cas1–3* (SALK_152551) were reconfirmed by DNA sequencing (SI Fig. 10). (*B*) RNA gel blot analysis. To verify equal loading and transfer efficiency of RNA, the membrane was stained with methylene blue (*Lower*). The hybridization signal with a radioactively labeled probe prepared with *CAS1* cDNA is presented (*Upper*). Positions of the wild-type mRNA and chimeric *CAS1-NPTII* transcript expressed from the *cas1–1* locus are indicated. (*C*) RT-PCR analysis. cDNAs were synthesized with reverse transcriptase and RNA from samples analyzed in *B*. These cDNAs served as templates in the PCRs with Pr1 and Pr2 shown in *A*. CAS1 isoforms encoded by alternatively spliced transcripts in the *cas1–1* mutant are shown on the right (SI Table 2).

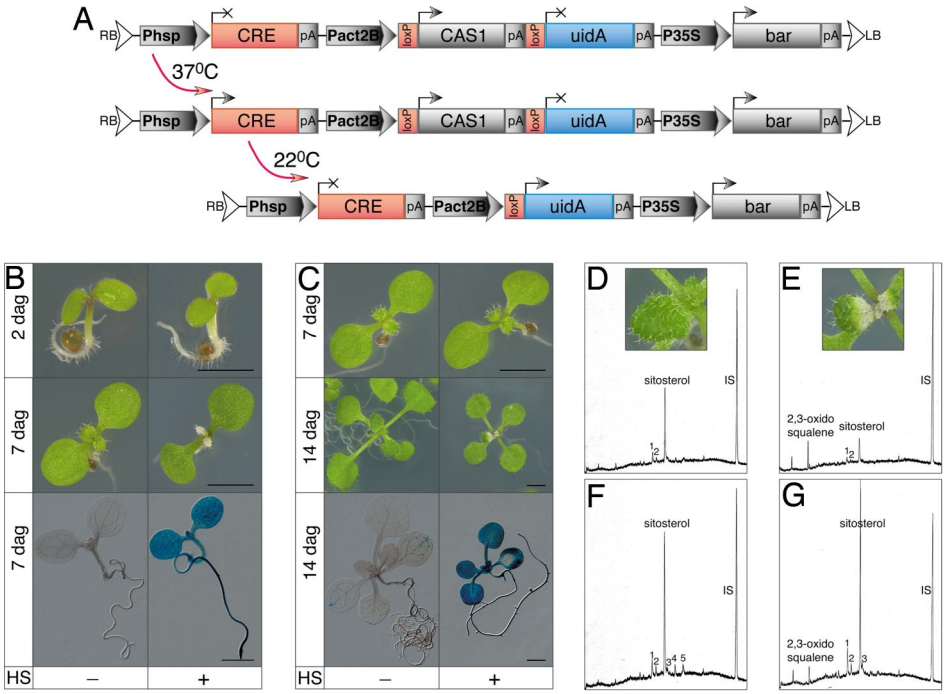


**Fig. 6.** Generation and analysis of the conditional *cas1–2* mutant allele. (*A*) Design of the *cas1–2* mutation-complementing vector pCRECAS1 and sequence of events *in planta* after heat shock. Elements are promoters ($P_{hsp}$, $P_{act2B}$, $P_{35S}$), protein-coding regions (CRE, CAS1, uidA, bar), mRNA polyadenylation sequences (pA), and *loxP* sites (loxP); LB and RB are border sequences delineating the DNA transferred (T-DNA) into plant cells from *Agrobacterium tumefaciens.* Arrows or crosses indicate expression or lack of expression of gene(s). (*B*) Requirement of CAS1 for plastid differentiation and leaf growth. Two days after germination on a standard synthetic medium, seedlings were heat stressed (HS) at 37°C for 6 h (+) and then grown under standard conditions. Non-HS seedlings (−) are on the left. Phenotypes of seedlings and GUS-staining patterns 7 days after germination (dag) are shown. (*C*) Assessment of the role of *CAS1* in cells with differentiated plastids. Seedlings bearing visible first leaf pairs were HS (+), photographed at 14 dag, and stained for GUS activity, along with control (−) plants. (*D–G*) Sterol analysis. Post-HS neoformed tissues (i.e., distal half of root, second leaf pair, and proximal half of leaves from first pair) and HS-preformed tissues (i.e., proximal half of root, cotyledons and hypocotyls, and distal half of leaves from first pair) were sampled from 25 seedlings of the wild-type and of the *cas1–2* conditional allele in three independent experiments. GC of crude hexanic extracts of nonsaponifiable lipids gave profiles typical of plants with *CAS1* (*D*) and *cas1–2* (*E*) phenotypes in the case of neoformed tissues and profiles typical of plants with *CAS1* (*F*) and *cas1–2* phenotypes (*G*) in the case of preformed tissues. The *Insets* in *D* and *E* demonstrate that HS (+) wild-type and *cas1–2* conditional allele had the same growth stage. Chromatograms obtained with the Agilent 6890 GC device show data acquisition after 20 min and until 52 min of the runs. Major peaks are sitosterol and 2,3-oxidosqualene (Fig. 1). Other sterol compounds identified by their mass spectrum are: 1, campesterol; 2, stigmasterol; 3, isofucosterol; 4, cycloartenol; and 5, 24-methylene cycloartenol. IS, internal standard (lupenyl-diacetate) present in identical amount in each sample. (Scale bars, 2 mm.)

To address this question, we analyzed the knockout mutant alleles *cas1–2* (SALK_119879) and *cas1–3* (SALK_152551) (29) that were caused by T-DNA insertions in the seventh exon and in the ninth intron of *CAS1*, respectively (Fig. 5*A* and SI Fig. 10). No homozygous mutant plants were found among 50 individuals of a self-progeny of either *CAS1/cas1–2* or *CAS1/cas1–3*. Analysis of 50 plants per progeny from reciprocal crosses between heterozygous *CAS1/cas1–2(cas1–3)* and wild-type *CAS1/CAS1* plants revealed that *CAS1/cas1–2(cas1–3)* progenies were obtained only if *CAS1/cas1–2(cas1–3)* was used as a female in the cross. Consequently, these two T-DNA insertions caused a male-specific transmission defect, suggesting that the protein is essential for the male gametophyte function.

To characterize the function of CAS1 in postgametophytic plant development, we used a *CRE/loxP* method for a mosaic analysis in the *Arabidopsis cas1–2* background (30). The design of the gene construct used, pCRECAS1, is schematically presented in Fig. 6*A*. Approximately 10% of the primary transformants (T1) generated with pCRECAS1 had abnormal phenotypes that could be categorized into three classes (SI Fig. 11): in one class, plants had albino stems, resembling *cas1–1* mutant plants; in a second class, plants were characterized by green leaves with albino bases and petioles; and in the third group, leaf shape and pigmentation were abnormal. Most probably, these mutant phenotypes among the T1 plants were attributable to the DNA homology-dependent cosuppression of the endogenous *CAS1* gene (31). T1 lines with abnormal phenotypes as such or in their progeny were excluded from the analysis. In the T2 progeny of the remaining 48 transgenic lines, *cas1–2/cas1–2* homozygous individuals were found, demonstrating that the $P_{ACT2}$::*CAS1*::*NOS* gene cassette complemented male-specific transmission defect. Five independent *cas1–2* homozygous transgenic lines (crecas2–1, crecas 2–4, crecas2–5, cre1, and cre38) were selected because they had constitutive *GUS* expression patterns after heat shock, indicating efficient CRE recombinase-mediated excision of the *CAS1* cDNA.

Induction of CAS1 loss of function resulted in a reproducible mutant phenotype. When 2-day-old seedlings were heat stressed, they developed small, narrow albino leaves 5 days after heat shock (DAHS) (Fig. 6*B*). In another example (Fig. 6*C*), 7-day-old seedlings with a well emerged first pair of true leaves at the time of heat shock application were analyzed. One week after heat shock, the growth of the first leaf pair that remained green was maintained in the plantlets. In contrast, the third and the fourth leaves were retarded in their development, and their bases were albino, whereas the fifth leaf was very small and purely albino. No other macroscopically discernible leaves appeared during the following 2 weeks of culture, suggesting that the shoot apical meristem activity was terminated. Similarly to leaves, roots of heat-stressed seedlings ceased their growth 5 to 7 DAHS. Albino tissues also turned necrotic and died ≈10–14 DAHS. To verify that the observed mutant phenotypes were caused by the CAS1 loss of function, we compared the composition of hexane extracts of nonsaponifiable lipids in heat-stressed and control plants by GC. Only plantlets from the *cas1–2* conditional allele that had experienced heat shock

during their growth accumulated 2,3-oxidosqualene (compare chromatograms in Fig. 6 *E* vs. *D* and *G* vs. *F*). In addition, tissues of the *cas1–2* conditional allele that developed after the heat shock and displayed albinism contained a lower amount of the pathway end products than the wild-type counterpart tissues that had experienced the same heat shock. Thus, the induction of the CAS1 loss of function by using the conditional heat shock-inducible *cas1–2* allele resulted in cessation of chloroplast differentiation in newly growing leaves, accompanied by growth arrest and followed by the death of bleached tissue.

## Discussion

We describe here the defective male-specific transmission of *cas1–2* and *cas1–3* mutant alleles, as well as abnormal growth of leaves and the arrest of shoot and root meristems in induced loss-of-function *cas1–2* seedlings. These phenotypes are most probably a consequence of structural defects in cellular membrane networks caused by the measured depletion of sterols. This conclusion is consistent with studies in yeast and animal cells revealing that sterols are essential components of cell membranes and that their concentration is tightly controlled by a feedback system that operates at transcriptional and posttranscriptional levels (32). Thus, CAS1 is required for the plant cell viability, and its function is not redundant with other 2,3-oxidosqualene cyclases of *Arabidopsis*.

Analysis of the weak *cas1–1* and conditional *cas1–2* mutant alleles revealed a role for CAS1 in plastid biogenesis. At the cellular level, albino phenotypes in plants can be caused both by an abortion in biogenesis of the plastidial thylakoid membrane, where chlorophyll–protein complexes accumulate, and by a photooxidative damage to developing thylakoid membranes because of suboptimal production of photoprotective carotenoids. Stability of chlorophyll–protein complexes depends on the availability of lipids (33); however, sterols have not been reported as components of plastid membranes (34). Biogenesis of thylakoids requires extensive exchange, the so-called lipid trafficking, of lipid precursors between the chloroplast and the endoplasmic reticulum (ER) (33). These two cellular compartments develop contact sites between the outer plastid envelope and the sterol-rich ER membranes (35). Unbalanced sterol composition and sterol depletion identified in *cas1* mutants could compromise ER–plastid physical contacts.

On the other hand, we found that the *cas1–1* albino phenotype is conditionally light-dependent, which correlates with a defect in accumulation of carotenoids. Carotenoids are end products of the plastidial terpenoid biosynthetic pathway, whereas sterols are end products of the cytosolic terpenoid pathway. Albinism of *cas1* mutants may represent genetic evidence for a regulatory mechanism that is thought to coordinate activity of compartmentalized terpenoid biosynthesis in the plant cell (36).

## Materials and Methods

**Plant Growth.** Seeds of *Arabidopsis thaliana* (L.) Heyhn. were sown in a standard soil compost mixture, and seedlings were grown individually in growth chambers under white fluorescent lamps. Photon fluency was 40–60 $\mu mol \cdot m^{-2} \cdot s^{-1}$ at the rosette level and 70–90 $\mu mol \cdot m^{-2} \cdot s^{-1}$ at that of inflorescence tips, i.e., ≈20–30 cm above the rosettes. The temperature was 22°C during the day (12 h) and 19°C during the night (12 h).

**Molecular Analysis of Nucleic Acids.** Total RNA was isolated and analyzed by RNA gel blot hybridization (37). For RT-PCR analysis, total RNA was treated with DNaseI and additionally purified with an RNeasy kit (Qiagen). The oligo(dT)-primed first-strand cDNA was synthesized on 5 $\mu$g of total RNA with thermoscript reverse polymerase (Invitrogen). Chimeric cDNAs of *CAS1* and the neomycin phosphotransferase II-encoding gene (*NPTII*) were amplified by PCR with Taq DNA polymerase (Roche Molecular Biochemicals) and the *CAS1*-specific primer Pr1 (primer 1; 5′-GGCTATGCTCGCACTCATTGGT-3′), and *NPTII*-specific primer Pr2 (primer 2; 5′-CCCCTGCGCTGACAGCCGGAACACG-3′) (Fig. 5*A*). Amplified DNA fragments were subcloned into pCRTOPO (Invitrogen) for DNA sequence analysis.

**Construction of a Conditional *cas1–2* Allele.** The details of the preparation of the binary vector pCRECAS1 are available upon request. Elements incorporated into this vector were the vector backbone from a binary vector pPZP200 (38); a plant selectable marker conferring resistance to glufosinate-ammonium (BASTA) as a CaMV 35S promoter driving the expression of the *BAR* gene (39); the heat shock promoter from *AtHSP18.2* (40) and octopine synthase polyadenylation sequences to drive the expression of the *CRE-intron* gene (41); the promoter of the *At3g18780* that encodes ACTIN2 (42); and the nopaline synthase polyadenylation sequences used to drive the expression of the *CAS1* cDNA. Progenies of transformed *CAS1/cas1–2* plants were screened for individuals resistant to BASTA that were genotyped by PCR for plants homozygous for the SALK_119879 *cas1–2* knockout mutant allele (*SI Methods*).

**Triterpenoid Analysis.** Samples were collected, freeze-dried, and ground with an Ultra-Turrax blender (Janke und Künkel, IKA Labortechnik) in 15–25 ml of 6% KOH in MeOH at 80°C for 2 h. The nonsaponifiable compounds were extracted with three volumes of *n*-hexane and separated on silica TLC plates (0.25 mm thickness; Merck) with two runs of dichloromethane. 2,3-Oxidosqualene was scraped off the plate ($R_f = 0.6$) and identified by comparison with an authentic standard of 2,3-oxidosqualene (racemic) (6*E*,10*E*,14*E*,18*E*)-2,3-epoxy-2,6,10,15,19,23-hexamethyl-6,10,14,18,22-tetracosapentaene ($C_{30}H_{50}O$) (Echelon Biosciences Laboratories) and sterols as acetate derivatives with a 8200 gas chromatograph (Varian) equipped with a DB-1 column as described (4, 14, 26). Lupenyl-3,28-diacetate was added to the extract of nonsaponifiable compounds as an internal standard for quantification of 2,3-oxidosqualene and total triterpenoids (sterols and triterpenes). Identification of compounds was confirmed by GC/MS with a 6890 gas chromatograph (Agilent) equipped with a DB-5MS column (J&W; 30 m long, 0.32 mm i.d., 0.25-$\mu$m film thickness) coupled with a 5973 mass selective detector (Agilent). The temperature program included a steep ramp from 60 to 220°C at 30°C per minute, followed by a 2°C per minute ramp from 220 to 300°C and a plateau at 300°C (He as carrier gas, 2 ml/min).

**Measurement of HMGR Activity.** Membranes from *Arabidopsis* tissues were isolated as described (43). Microsomal proteins were quantified by the Bio-Rad protein assay with BSA as a standard. The standard HMGR assay consisted of 100 mM $K_2PO_4$, pH 7.5, 4.2 mM EDTA, 8.4 mM DTE, 100 $\mu$g BSA, 600 $\mu$M NADPH, and 30 $\mu$M (0.1 $\mu$Ci) (R,S)-[3-$^{14}$C]3-hydroxy-3-methylglutaryl-CoA in a final volume of 60 $\mu$l, incubated, and processed as described (25, 26) (*SI Methods*).

**ACKNOWLEDGMENTS.** We thank Professors Pierre Benveniste and Dirk Inzé for encouragement; Yves Poirier, Michel Rohmer, Thomas Bach, and Jacques-Henry Weil for comments and advice; Màrta Ramel for horticultural work; Riet De Rycke for help with the microscopical analysis; Karel Spruyt and Pascal Disdier for photographic work; and Martine De Cock for help in preparing the manuscript. The Arabidopsis Biological Resource Center (Ohio State University) is acknowledged for providing T-DNA insertional mutant lines. This work was supported by Centre National de la Recherche Scientifique and Agence Nationale de la Recherche Grant TERPENE ANR-05-BLAN-0217-02 (to V.C.) and by European Union Grant EXOTIC QLG2-CT-1999-000351 (to S.K.).

1. Benveniste P (1986) Sterol biosynthesis. *Annu Rev Plant Physiol* 37:275–308.
2. Benveniste P (2004) Biosynthesis and accumulation of sterols. *Annu Rev Plant Biol* 55:429–457.
3. Corey EJ, Matsuda SPT, Bartel B (1993) Isolation of an *Arabidopsis thaliana* gene encoding cycloartenol synthase by functional expression in a yeast mutant lacking lanosterol synthase by the use of a chromatographic screen. *Proc Natl Acad Sci USA* 90:11628–11632.
4. Husselstein-Muller T, Schaller H, Benveniste P (2001) Molecular cloning and expression in yeast of 2,3-oxidosqualene-triterpenoid cyclases from *Arabidopsis thaliana*. *Plant Mol Biol* 45:75–92.
5. Kolesnikova MD, Xiong Q, Lodeiro S, Hua L, Matsuda SPT (2006) Lanosterol biosynthesis in plants. *Arch Biochem Biophys* 447:87–95.
6. Suzuki M, *et al.* (2006) Lanosterol synthase in dicotyledonous plants. *Plant Cell Physiol* 47:565–571.
7. Phillips DR, Rasbery JM, Bartel B, Matsuda SPT (2006) Biosynthetic diversity in plant triterpene cyclization. *Curr Opin Plant Biol* 9:305–314.
8. Herrera JBR, Bartel B, Wilson WK, Matsuda SPT (1998) Cloning and characterization of the *Arabidopsis thaliana* lupeol synthase gene. *Phytochemistry* 49:1905–1911.
9. Kushiro T, Shibuya M, Ebizuka Y (1998) $\beta$-Amyrin synthase. Cloning of oxidosqualene cyclase that catalyzes the formation of the most popular triterpene among higher plants. *Eur J Biochem* 256:238–244.
10. Segura MJR, Meyer MM, Matsuda SPT (2000) *Arabidopsis thaliana* LUP1 converts oxidosqualene to multiple triterpene alcohols and a triterpene diol. *Org Lett* 2:2257–2259.

11. Ebizuka Y, Katsube Y, Tsutsumi T, Kushiro T, Shibuya M (2003) Functional genomics approach to the study of triterpene biosynthesis. *Pure Appl Chem* 75:369–374.
12. Fazio GC, Xu R, Matsuda SPT (2004) Genome mining to identify new plant triterpenoids. *J Am Chem Soc* 126:5678–5679.
13. Schrick K, *et al.* (2000) FACKEL is a sterol C-14 reductase required for organized cell division and expansion in *Arabidopsis* embryogenesis. *Genes Dev* 14:1471–1484.
14. Kim HB, *et al.* (2005) Arabidopsis *cyp51* mutant shows postembryonic seedling lethality associated with lack of membrane integrity. *Plant Physiol* 138:2033–2047.
15. Li J, Nagpal P, Vitart V, McMorris TC, Chory J (1996) A role for brassinosteroids in light-dependent development of *Arabidopsis. Science* 272:398–401.
16. Klahre U, *et al.* (1998) The Arabidopsis *DIMINUTO/DWARF1* gene encodes a protein involved in steroid synthesis. *Plant Cell* 10:1677–1690.
17. Choe S, *et al.* (1999) The Arabidopsis *dwf7/ste1* mutant is defective in the $\Delta^7$ sterol C-5 desaturation step leading to brassinosteroid biosynthesis. *Plant Cell* 11:207–221.
18. Schaeffer A, Bronner R, Benveniste P, Schaller H (2001) The ratio of campesterol to sitosterol that modulates growth in *Arabidopsis* is controlled by *STEROL METHYLTRANSFERASE 2;1*. *Plant J* 25:605–615.
19. Carland FM, Fujioka S, Takatsuto S, Yoshida S, Nelson T (2002) The identification of *CVP1* reveals a role for sterols in vascular patterning. *Plant Cell* 14:2045–2058.
20. Rasbery JM, *et al.* (2007) *Arabidopsis thaliana* squalene epoxidase 1 is essential for root and seed development. *J Biol Chem* 282:17002–17013.
21. Clouse SD (2002) Arabidopsis mutants reveal multiple roles for sterols in plant development. *Plant Cell* 14:1995–2000.
22. Lindsey K, Pullen ML, Topping JF (2003) Importance of plant sterols in pattern formation and hormone signalling. *Trends Plants Sci* 8:521–525.
23. Schaller H (2003) The role of sterols in plant growth and development. *Prog Lipid Res* 42:163–175.
24. Babiychuk E, Fuangthong M, Van Montagu M, Inzé D, Kushnir S (1997) Efficient gene tagging in *Arabidopsis thaliana* using a gene trap approach. *Proc Natl Acad Sci USA* 94:12722–12727.
25. Gondet L, Weber T, Maillot-Vernier P, Benveniste P, Bach TJ (1992) Regulatory role of microsomal 3-hydroxy-3-methylglutaryl-coenzyme A reductase in a tobacco mutant that overproduces sterols. *Biochem Biophys Res Commun* 186:888–893.
26. Schaller H, *et al.* (1995) Expression of the *Hevea brasiliensis* (HBK.) Müll. Arg. 3-hydroxy-3-methylglutaryl-coenzyme A reductase 1 in tobacco results in sterol overproduction. *Plant Physiol* 109:761–770.
27. Chappell J, Wolf F, Proulx J, Cuellar R, Saunders C (1995) Is the reaction catalyzed by 3-hydroxy-3-methylglutaryl coenzyme A reductase a rate-limiting step for isoprenoid biosynthesis in plants? *Plant Physiol* 109:1337–1343.
28. Suzuki M, *et al.* (2004) Loss of function of *3-hydroxy-3-methylglutaryl coenzyme A reductase 1* (*HMG1*) in *Arabidopsis* leads to dwarfing, early senescence and male sterility, and reduced sterol levels. *Plant J* 37:750–761.
29. Alonso JM, *et al.* (2003) Genome-wide insertional mutagenesis of *Arabidopsis thaliana. Science* 301:653–657.
30. Sieburth LE, Drews GN, Meyerowitz EM (1998) Non-autonomy of *AGAMOUS* function in flower development: Use of a Cre/*loxP* method for mosaic analysis in *Arabidopsis. Development* 125:4303–4312.
31. Qin H, Dong Y, von Arnim AG (2003) Epigenetic interactions between *Arabidopsis* transgenes: Characterization in light of transgene integration sites. *Plant Mol Biol* 52:217–231.
32. Goldstein JL, DeBose-Boyd RA, Brown MS (2006) Protein sensors for membrane sterols. *Cell* 124:35–46.
33. Awai K, Xu C, Lu B, Benning C (2006) Lipid trafficking between the endoplasmic reticulum and the chloroplast. *Biochem Soc Trans* 34:395–398.
34. Melkonian M, Robenek H, Steup M (1981) Occurrence and distribution of filipin-sterol complexes in chloroplast envelope membranes of algae and higher plants as visualized by freeze-fracture. *Protoplasma* 109:349–358.
35. Andersson MX, Goksör M, Sandelius AS (2007) Optical manipulation reveals strong attracting forces at membrane contact sites between endoplasmic reticulum and chloroplasts. *J Biol Chem* 282:1170–1174.
36. Laule O, *et al.* (2003) Crosstalk between cytosolic and plastidial pathways of isoprenoid biosynthesis in *Arabidopsis thaliana*. *Proc Natl Acad Sci USA* 100:6866–6871.
37. Babiychuk E, Kushnir S, Belles-Boix E, Van Montagu M, Inzé D (1995) *Arabidopsis thaliana* NADPH oxidoreductase homologs confer tolerance of yeasts toward the thiol-oxidizing drug diamide. *J Biol Chem* 270:26224–26231.
38. Hajdukiewicz P, Svab Z, Maliga P (1994) The small, versatile *pPZP* family of *Agrobacterium* binary vectors for plant transformation. *Plant Mol Biol* 25:989–994.
39. Hellens RP, Edwards EA, Leyland NR, Bean S, Mullineaux PM (2000) pGreen: A versatile and flexible binary Ti vector for *Agrobacterium*-mediated plant transformation. *Plant Mol Biol* 42:819–832.
40. Matsuhara S, Jingu F, Takahashi T, Komeda Y (2000) Heat-shock tagging: A simple method for expression and isolation of plant genome DNA flanked by T-DNA insertions. *Plant J* 22:79–86.
41. Joubès J, De Schutter K, Verkest A, Inzé D, De Veylder L (2004) Conditional, recombinase-mediated expression of genes in plant cell cultures. *Plant J* 37:889–896.
42. An Y-Q, *et al.* (1996) Strong, constitutive expression of the *Arabidopsis ACT2/ACT8* actin subclass in vegetative tissues. *Plant J* 10:107–121.
43. Du L, Lykkesfeldt J, Olsen CE, Halkier BA (1995) Involvement of cytochrome P450 in oxime production in glucosinolate biosynthesis as demonstrated by an *in vitro* microsomal enzyme system isolated from jasmonic acid-induced seedlings of *Sinapis alba* L. *Proc Natl Acad Sci USA* 92:12505–12509.